← click for updates

Small-scale universality in fluid turbulence

Jörg Schumacher[a], Janet D. Scheel[b], Dmitry Krasnov[a], Diego A. Donzis[c], Victor Yakhot[d], and Katepalli R. Sreenivasan[e,1]

[a]Department of Mechanical Engineering, Technische Universität Ilmenau, D-98684 Ilmenau, Germany; [b]Department of Physics, Occidental College, Los Angeles, CA 90041; [c]Department of Aerospace Engineering, Texas A&M University, College Station, TX 77843; [d]Department of Aerospace and Mechanical Engineering, Boston University, Boston, MA 02215; and [e]Departments of Physics and Mechanical Engineering, and the Courant Institute of Mathematical Sciences, New York University, New York, NY 10012

Turbulent flows in nature and technology possess a range of scales. The largest scales carry the memory of the physical system in which a flow is embedded. One challenge is to unravel the universal statistical properties that all turbulent flows share despite their different large-scale driving mechanisms or their particular flow geometries. In the present work, we study three turbulent flows of systematically increasing complexity. These are homogeneous and isotropic turbulence in a periodic box, turbulent shear flow between two parallel walls, and thermal convection in a closed cylindrical container. They are computed by highly resolved direct numerical simulations of the governing dynamical equations. We use these simulation data to establish two fundamental results: (*i*) at Reynolds numbers Re ∼ 10^2 the fluctuations of the velocity derivatives pass through a transition from nearly Gaussian (or slightly sub-Gaussian) to intermittent behavior that is characteristic of fully developed high Reynolds number turbulence, and (*ii*) beyond the transition point, the statistics of the rate of energy dissipation in all three flows obey the same Reynolds number power laws derived for homogeneous turbulence. These results allow us to claim universality of small scales even at low Reynolds numbers. Our results shed new light on the notion of when the turbulence is fully developed at the small scales without relying on the existence of an extended inertial range.

fluid dynamics | energy dissipation rate

An enduring notion in the phenomenology of turbulence is the universality of small scales. It has been taken for granted in theoretical approaches (e.g., refs. 1–8) and analyzed in numerical simulations (9–11) as well as various laboratory experiments (e.g., refs. 5 and 12). The standard paradigm is that whereas the large scales are nonuniversal, reflecting the circumstances of their generation, an increasingly weaker degree of nonuniversality is imparted to small scales with increasing separation between the large and small scales. This scale separation is thought to increase with the flow Reynolds number, so a proper test of universality has been thought to require very high Reynolds numbers. Consequently, many substantial efforts have been made to produce such high-Reynolds-number flows (e.g., ref. 12).

Here, we show evidence for an alternative point of view: If one resolves small scales accurately, one observes, even at low Reynolds numbers, universal scaling of velocity gradients that manifest primarily at small scales. We stress that small-scale dynamics are strongly nonlinear even in low-Reynolds-number flows driven by large-scale forcing. There is thus considerable merit in measuring or simulating low-Reynolds-number flows much more accurately than has been the practice and exploring the evidence for universality (or lack thereof), instead of advancing as inevitable the notion that useful lessons about universality are possible only at very high Reynolds numbers. Indeed, another result of this paper is that there exists a threshold Reynolds number above which Gaussian-like fluctuations tend to assume intermittent characteristics of fully developed flows and that these features can be extracted by accessing increasingly smaller scales even if the Reynolds numbers are quite moderate. The latter result is especially important for purposes of identifying a fixed point in certain renormalization group expansion procedures (8).

Three Turbulent Flows with Increasing Complexity

Our study is based on three turbulent flows of systematically increasing complexity (homogeneous and isotropic turbulence in a periodic box, flow between two parallel walls, and thermal convection in a closed cylindrical container) that are computed by well-resolved direct numerical simulations. All these flows are governed by the Navier–Stokes equations

$$\frac{\partial u_i}{\partial x_i} = 0, \qquad [1]$$

$$\frac{\partial u_i}{\partial t} + u_j \frac{\partial u_i}{\partial x_j} = -\frac{1}{\rho} \frac{\partial p}{\partial x_i} + \nu \frac{\partial^2 u_i}{\partial x_j^2} + f_i, \qquad [2]$$

where ν is the kinematic viscosity, p is the pressure, ρ is the mass density, and the forcing $f_i(x_j, t)$ stands for different mechanisms of maintaining the turbulence. For the convection problem an additional advection–diffusion equation has to be solved for the temperature field $T(x_j, t)$ that couples back to the flow via the forcing term f_i. The turbulent velocity field $u_i(x_j, t)$ is decomposed into a fluctuating component $v_i(x_j, t)$ and a mean flow $\overline{u}_i(x_j)$. We define the Reynolds number as

$$\mathrm{Re} = \frac{v_{\mathrm{rms}} L}{\nu}, \qquad [3]$$

where v_{rms} is the root-mean-square fluctuation velocity; the length scale L is the side of the cube for box turbulence (9), half the distance H for the turbulent shear flow between parallel plates (13) and the height H of the cell for convection (14, 15).

Different boundary conditions and forcing produce different large-scale features. The simplest of these three flows is the homogeneous isotropic turbulent flow in a cube with periodic

Significance

Since the time Kolmogorov postulated the universality of small-scale turbulence, an important research topic has been to experimentally establish it beyond doubt. The likelihood of small-scale universality increases with increasing distance (say, in wave number space) from the nonuniversal large scales. This distance increases as some power of the flow Reynolds number, and so a great deal of emphasis has been put on creating and quantifying very high Reynolds number flows under controlled conditions. The present paper shows that the universal properties of inertial range turbulence (thought to exist only at very high Reynolds numbers) are already present in an incipient way even at modest Reynolds numbers and hence changes the paradigm of research in this field.

PHYSICS

boundaries and without a mean flow (Fig. 1*A*). The turbulence here is sustained by forcing at the large scale (9, 10). In ref. 9 a handful of low-wavenumber Fourier modes is driven such that a fixed amount of turbulent kinetic energy is injected into the flow at each time unit. Some details of these procedures are discussed in *SI Text*. In ref. 10, a stochastic forcing is applied for a number of low-wavenumber Fourier modes. Statistical homogeneity is established in all three space directions. Next in complexity is the flow between parallel plates with no-slip boundaries (Fig. 1*B*) and a mean flow $\bar{u}_x(z)$ (13), where z is in the direction separating the plates. The turbulence is inhomogeneous in direction z but homogeneous in the downstream direction x along the flow because of the constant pressure drop and also, by construction, in the spanwise direction y. Statistical homogeneity in the azimuthal direction remains in a cylindrical Rayleigh–Bénard convection (RBC) cell with solid walls (Fig. 1*C*). This turbulent flow, also satisfying the no-slip condition on all of the walls, is driven by a sustained temperature difference ΔT between the top and bottom plates that causes buoyancy forces to trigger and maintain the fluid motion (14, 15). The side walls are thermally insulated. In the Boussinesq approximation (16), the driving simplifies to $f_z = g\alpha T$, with gravity acceleration g and (isobaric) thermal expansion coefficient α. Here the mean flow is a large-scale 3D circulation whose scale is comparable to the cell size (17–19).

At the smallest scales in a turbulent flow the kinetic energy is dissipated into frictional heat by molecular viscosity. The amount of kinetic energy loss per unit mass and unit time is the kinetic energy dissipation rate, which is defined as

$$\epsilon = \frac{\nu}{2}\left(\frac{\partial v_i}{\partial x_j} + \frac{\partial v_j}{\partial x_i}\right)^2 . \qquad [4]$$

The statistical mean of the energy dissipation rate, $\bar{\epsilon}$, is also the rate of energy transfer from large scales of the order L down to the smallest ones on the order of the viscous scales $\eta_K = \nu^{3/4}/\varepsilon^{-1/4}$, at which the velocity fluctuations are damped out (1). Intermittent fluctuations of ε are displayed in Fig. 1 *D–F*, where we plot

instantaneous 2D slices of the field in logarithmic levels of intensity. In all three flows, we observe strongly filamented shear layers, a fingerprint of the spatial intermittency of the kinetic energy dissipation rate field.

We have collected data from direct numerical simulations of homogeneous isotropic box turbulence (9, 10) and channel flow turbulence (13) that apply the pseudospectral Fourier and Fourier–Chebyshev methods, respectively. These two methods are standard and need no elaboration. The third dataset for turbulent convection has been obtained with a spectral element method, the nek5000 package (20), which has been adapted to our turbulent convection study (21). In turbulent convection the temperature difference ΔT sustained between the hot bottom and the cold top plates is quantified nondimensionally by the Rayleigh number Ra = $g\alpha\Delta TH^3/(\nu\kappa)$, where κ is the thermal diffusivity of the fluid. The Prandtl number is set to that of convection in air or other gases with Pr = ν/κ = 0.7. Rayleigh numbers in our simulations vary over nearly five orders of magnitude from Ra = 3×10^5 to 10^{10}. The aspect ratio of the cylindrical cell is $\Gamma = D/H = 1$. The total number of mesh cells grows to more than 4 billion in all three flow cases, which requires massively parallel supercomputations (more details in *SI Text*).

Universal Scaling and Transition to Intermittency

Starting from the Navier–Stokes Eqs. **1** and **2**, the scaling relations for the moments of the energy dissipation rate were derived from a theory for homogeneous and isotropic turbulence in ref. 6. They are given by

$$\overline{\epsilon^n} \propto \mathrm{Re}^{d_n}, \qquad [5]$$

with the exponents

$$d_n = n + \frac{\zeta_{4n}}{\zeta_{4n} - \zeta_{4n+1} - 1}. \qquad [6]$$

Here, ζ_n is the inertial-range scaling exponent of the nth order moment of the velocity increment $\Delta_r v_x = v_x(x+r) - v_x(x)$, with v_x
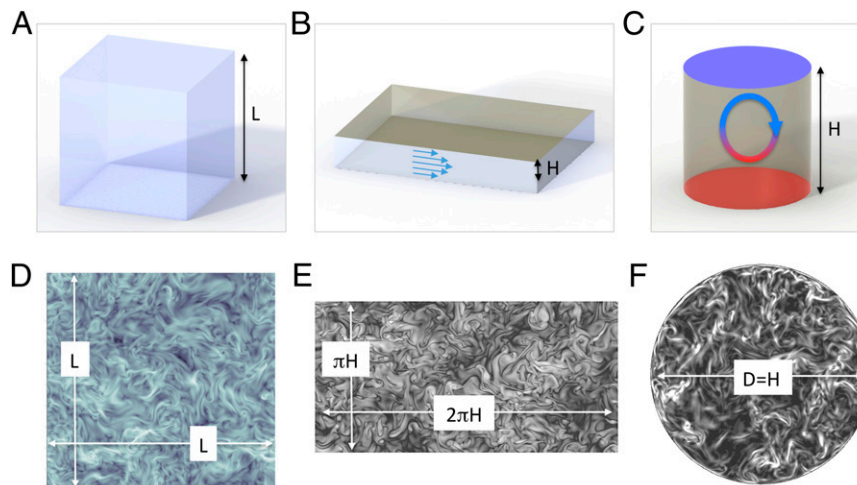
Fig. 1. Three turbulent flows and structure of energy dissipation field. (*A*) Homogeneous and isotropic turbulence in a cube of length L on the side with periodic boundary conditions in all three space directions. Statistical homogeneity is present in all directions. (*B*) Turbulent shear flow in a channel of height $2H$ with solid walls at the top and bottom and periodic boundaries in the horizontal directions. The unidirectional mean flow in the downstream direction is indicated and homogeneity is sustained in both horizontal directions. (*C*) Cylindrical convection cell of height H and radius R with isothermal hot bottom and cold top plate. The cell of unit aspect ratio is given by $V = \{(r, \phi, z): 0 \le r/R \le 0.5; 0 \le z/H \le 1\}$. The mean flow, a 3D large-scale circulation, is shown schematically (see description of Fig. 2*B*). The convective flow in the cylindrical cell is statistically homogeneous in the azimuthal direction only. (*D*) A slice (parallel to one of the walls) of the instantaneous kinetic energy dissipation rate field for Re = 5,587 in box turbulence (10). The box with a side length $L = 2\pi$ was resolved with $2,048^3$ equidistant grid points. (*E*) Kinetic energy dissipation rate in the midplane of a channel flow for Re = 1,160. The simulation required $2,048 \times 2,049 \times 1,024$ points for a channel with spatial extent $2\pi H \times 2H \times \pi H$. (*F*) Same quantity in the midplane of a convection cell at Re = 4,638. The convection cell of unit aspect ratio is covered by 875,520 spectral elements, each containing 12^3 Gauss–Lobatto–Legendre collocation points.

being the velocity fluctuation in the x direction and the separation distance r also measured along x (definition in *SI Text*). To make further progress, the functional dependence of the scaling exponents ζ_{2n} has to be given explicitly. In ref. 22 a convenient functional form with $\zeta_{2n} = 2n(1 + 3\beta)/(3(1 + 2\beta n))$ is provided that, with the free-fitting parameter β set to 0.05, agrees with available experimental data in high-Reynolds-number flows (5) as well as with popular parameterizations of ζ_n, e.g., with the She–Lévêque intermittency model (4). This leads to $d_2 = 0.157$, $d_3 = 0.489$, and $d_4 = 0.944$. Additionally, $d_1 = 0$. Note that the fact $d_1 \leq 0$ has been proved from first principles (23). Higher exponents are beyond the reach of rigorous mathematics until the existence–uniqueness problem for the Navier–Stokes equations is solved (24).

The most important ingredient of the theory is the concept of a locally fluctuating scale η (25, 26), which probes local velocity gradients and is connected to the local velocity difference and viscosity by $\eta\Delta_\eta v_x = \nu$ (27, 28). The resulting theory yields a prediction that is different from that of the Kolmogorov refined similarity hypothesis (29): $d_n^{K62} = 3(n - \zeta_{3n})/4$ (30). The power law exponents d_n are connected with the exponents of the longitudinal velocity increment moments in the inertial range, $\overline{(\Delta_r v_x)^n} \propto r^{\zeta_n}$.

Definition [4] shows that the determination of the full dissipation field requires the measurement of all nine components of the velocity gradient tensor $\partial v_i / \partial x_j$, which is still a challenging experimental task (31). Numerical simulations also become very demanding because high-amplitude events of the energy dissipation field have to be resolved correctly (9). We have taken a computational mesh that is finer than in standard simulations, which enhances the computational effort significantly. The gain is a faithfully represented velocity gradient. The statistical convergence of the dissipation rate moments for the RBC case is discussed in *SI Text*. Many studies of homogeneous turbulence exist (e.g., refs. 10, 11, and 32) and, although fewer in number, also of channel flows (e.g., refs. 13, 33, and 34). The definition of the Reynolds number in each of these two cases is straightforward.

The definition of the Reynolds number Re in convection needs some thought. Fig. 2A shows Re as a function of the Rayleigh number (i.e., nondimensional thermal driving) for two choices of the velocity: the SD of the total velocity field, u_{rms}, and of the fluctuations, v_{rms}. The least-squares fits to both Reynolds numbers follow nearly the same scaling. What is important is to get a sense of the mean wind, or large-scale circulation, that exists in the flow. Fig. 2B displays this mean flow for a Rayleigh number of Ra = 10^7. It consists of a single circulation roll that fills the whole cell and obeys very slow dynamics with respect to time, which would require very long simulation runs, inaccessible with present capabilities.

The first important result concerns the transition between nearly Gaussian and intermittent non-Gaussian behaviors for the velocity gradient statistics. We demonstrate this transition for one longitudinal velocity derivative, $\partial v_x / \partial x$. As shown in Fig. 3 A and C, the probability density functions of $\partial v_x / \partial x$ change from being nearly Gaussian to fat-tailed ones as the Reynolds number increases. Data for isotropic box turbulence and convection are displayed. In Fig. 3 B and D, it is possible to infer a transition from Gaussian to anomalous scaling of the moments of $\partial v_x / \partial x$ (from 0 for the skewness and 3 for the flatness factor). Whereas the derivatives in homogeneous isotropic turbulence have been analyzed in the whole volume, the data points for the RBC simulation are collected in a subvolume $V_b \subset V$ in the center of the convection cell. It is given by $V_b = \{(r, \phi, z):0 \leq r/R \leq 0.3; 0.2 \leq z/H \leq 0.8\}$, where R is the radius of the convection cell.

Three comments are appropriate. First, as one may expect, higher-order moments than the third and the fourth show a sharper transition. Second, this transitional behavior is shared by all three flows considered here (two of which are shown). Therefore, we might reasonably surmise this feature to be universal. The result
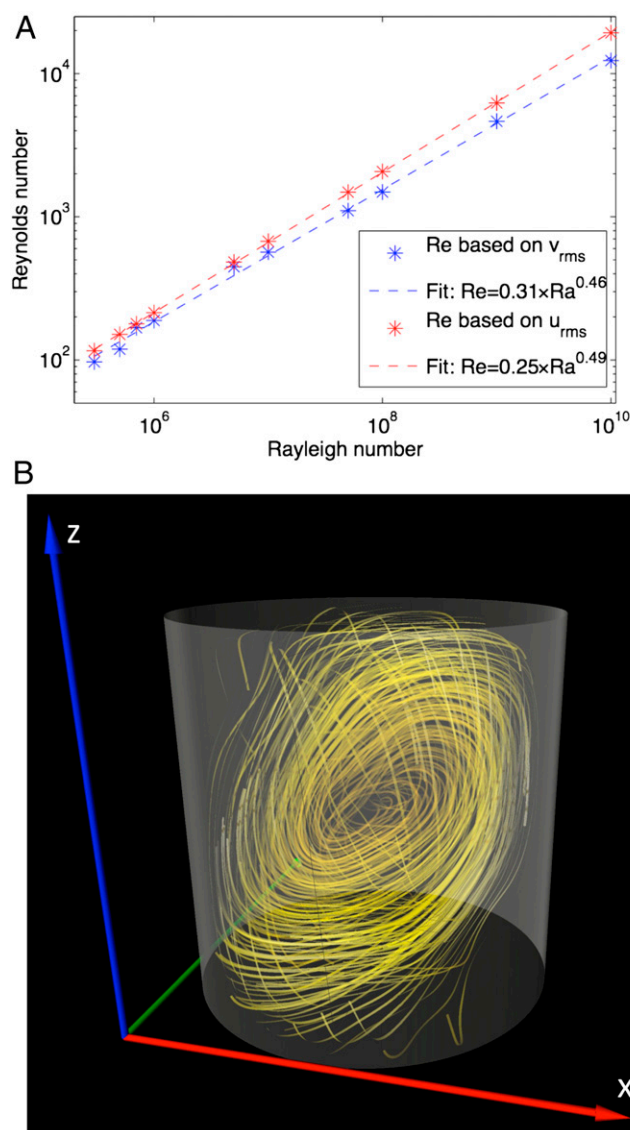
Fig. 2. Global flow conditions in inhomogeneous convective turbulence. (*A*) Reynolds number vs. Rayleigh number. Reynolds numbers are calculated using the full velocity field, u_i, and velocity fluctuations, v_i. The corresponding power law fits are shown as dashed lines. (*B*) Visualization of the 3D large-scale mean flow $\overline{u}_i(x_j)$ that is obtained by time averaging at Ra = 10^7.

on the transitional Reynolds number, previously underappreciated, is important because it provides a constraint on the development of turbulence models via renormalization group methods: It plays the role of the fixed point for calculations that repeatedly obliterate small scales by successive averaging protocols. Third, the transition Reynolds number, defined on the basis of the large scale in the flow, is on the order of 100 for all flows—although its precise numerical value depends on the forcing and other large-scale details.

In Fig. 4 we display the scaling of the dissipation rate moments of order $n = 2$–4 vs. the large-scale Reynolds number Re (error estimates in *SI Text*) and observe power-law scaling for all three flows, except for very low Reynolds numbers below transition. If one plots the data against Reynolds numbers after subtracting the transition values, the inference does not change substantially. The data points for isotropic box turbulence have been obtained by averaging over the whole volume. For the channel
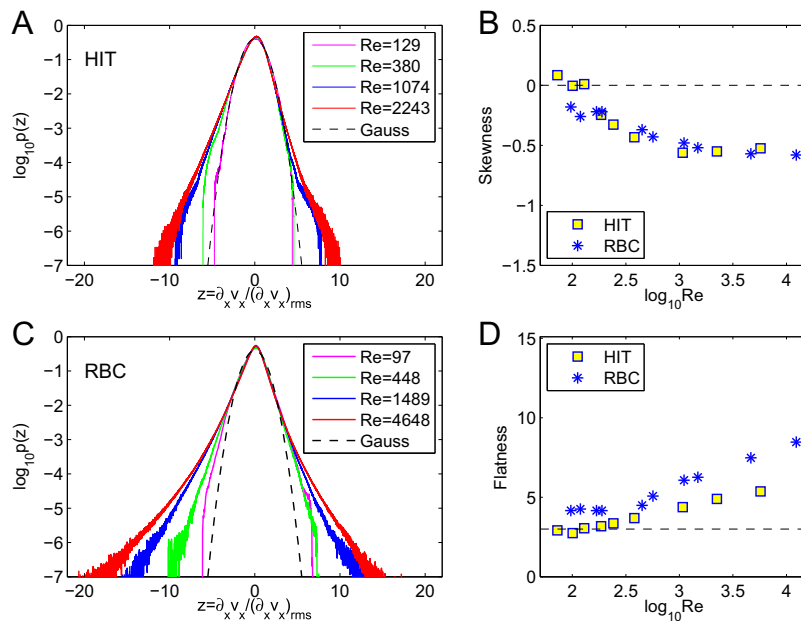
Fig. 3. Transition of velocity gradient statistics from Gaussian to super-Gaussian. Data are for homogeneous isotropic turbulence (HIT) and Rayleigh–Bénard convection (RBC). (*A*) Probability density functions of the longitudinal velocity derivative $\partial v_x / \partial x$ normalized by the corresponding root-mean-square at four different Reynolds numbers are displayed, $z = \partial v_x / \partial x / (\partial v_x / \partial x)_{rms}$. The Gaussian distribution is added as a dashed line for comparison. (*B*) Skewness $\overline{z^3} / \overline{z}^3$ of the longitudinal derivative z vs. Reynolds number Re (Eq. 3). (*C*) Same as *A*. Now four examples for the convection case are shown. (*D*) Flatness $\overline{z^4} / \overline{z}^4$ of the longitudinal derivative. In *B* and *D*, dashed lines are added, which indicate the skewness of zero and the flatness of three, respectively, which would hold for a Gaussian field. Velocity derivatives for the RBC analysis have been obtained in a bulk volume $V_b \subset V$ with $V_b = \{(r, \phi, z): 0 \le r/R \le 0.3; 0.2 \le z/H \le 0.8\}$. Velocity derivatives in isotropic turbulence have been collected in the whole volume.

flow averages were taken in a narrow slab around the center plane. The data points for the RBC simulation are collected again in the subvolume $V_b \subset V$ in the center of the convection cell. The interesting point is that the data follow the scaling predicted by the theory for homogeneous turbulence (6) for infinitely large Reynolds numbers, as indicated by dashed lines in Fig. 4 for each moment. This implies that the infinite-Re scaling, deduced theoretically for one flow, can be discerned at finite Re for all (three) flows. We believe that this is a powerful statement.

Discussion

We summarize our results as follows: For small Reynolds numbers of the order of 100, a transition occurs from sub-Gaussian or nearly Gaussian velocity gradient statistics to intermittent non-Gaussian ones. At the transition Reynolds number the derivative fluctuations are Gaussian. The existence of a Gaussian point is of theoretical interest in theories of renormalization (8). Past this transition point, velocity gradient statistics in all three flows follow a universal scaling behavior, as demonstrated here by the Reynolds number scaling of the energy dissipation rate ε. These results hold for three turbulent flows of increasing complexity, so we expect them to be universal. The sensitivity of this result to the large-scale forcing is yet to be understood in detail.

This study further suggests that the intermittent fluctuations of velocity gradients, which dominate at the lower end of the turbulent cascade range and down into the viscous range, display properties of high-Reynolds-number turbulence at much lower Reynolds number than is inferred from moments of velocity increments in the inertial range. In some sense, well-resolved dissipation contains ingredients of high-Reynolds-number turbulence once the transition value is exceeded.

These conclusions suggest also that, in the future, a plausible method for studying intermittent or anomalous scaling properties of turbulence is to study well-resolved energy dissipation at low to moderate Reynolds numbers, instead of chasing the goal

of "asymptotically high" values. This makes the turbulence problem entirely amenable to a serious study and opens alternative roads for the parameterization of small scales that cannot be resolved in many applications.
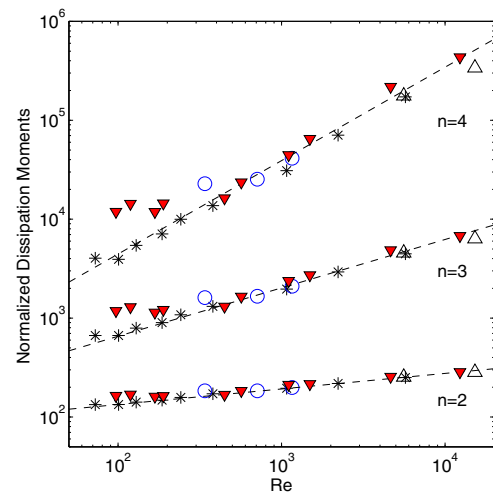
Fig. 4. Universality of the energy dissipation statistics. The Reynolds number dependence of normalized moments of orders $n = 2$, 3, and 4 of the energy dissipation rate, $\overline{\epsilon^n} / \overline{\epsilon}^n$, is compared for three turbulent flows. Black asterisks and white open triangles are for homogeneous isotropic turbulence data of refs. 9 and 10, respectively. Blue open circles are for turbulent channel flow (13) and red solid triangles are for turbulent Rayleigh–Bénard convection. Dashed lines correspond to a theoretical prediction by Yakhot (6) for the case of homogeneous isotropic turbulence (Fig. 1*A*). Datasets for different flows have been shifted vertically by constant factors to collapse the data records for the different orders. Data for RBC have been collected in subvolume V_b inside the cell.

1. Kolmogorov AN (1941) The local structure of turbulence in incompressible viscous fluid for very large Reynolds number. *Dokl Akad Nauk SSSR* 30:9–13.
2. Monin AS, Yaglom AM (1971) *Statistical Fluid Mechanics* (MIT Press, Cambridge, MA), Vol 2.
3. Frisch U (1994) *Turbulence* (Cambridge Univ Press, Cambridge, UK).
4. She Z-S, Lévêque E (1994) Universal scaling laws in fully developed turbulence. *Phys Rev Lett* 72(3):336–339.
5. Sreenivasan KR, Antonia RA (1997) The phenomenology of small-scale turbulence. *Annu Rev Fluid Mech* 29:435–472.
6. Yakhot V (2006) Probabilities in strong turbulence. *Physica D* 215(2):166–174.
7. Ruelle DP (2012) Hydrodynamic turbulence as a problem in nonequilibrium statistical mechanics. *Proc Natl Acad Sci USA* 109(50):20344–20346.
8. Yakhot V (2013) Reynolds number of transition as a dynamic constraint on statistical theory of turbulence. arXiv:1308.4205.
9. Schumacher J, Sreenivasan KR, Yakhot V (2007) Asymptotic exponents from low-Reynolds-number flows. *New J Phys* 9:89.
10. Donzis DA, Yeung PK, Sreenivasan KR (2008) Dissipation and enstrophy in isotropic turbulence: Resolution effects and scaling in direct numerical simulations. *Phys Fluids* 20:045108.
11. Ishihara T, Gotoh T, Kaneda Y (2009) Study of high-Reynolds number isotropic turbulence by direct numerical simulation. *Annu Rev Fluid Mech* 41:165–180.
12. Donnelly RJ, Sreenivasan KR (1998) *Flow at Ultra-High Reynolds and Rayleigh Numbers* (Springer, New York).
13. Hamlington PE, Krasnov D, Boeck T, Schumacher J (2012) Local dissipation scales and energy dissipation-rate moments in channel flow. *J Fluid Mech* 701:419–429.
14. Niemela JJ, Skrbek L, Sreenivasan KR, Donnelly RJ (2000) Turbulent convection at very high Rayleigh numbers. *Nature* 404(6780):837–840.
15. Shi N, Emran MS, Schumacher J (2012) Boundary layer structure in turbulent Rayleigh-Bénard convection. *J Fluid Mech* 706:5–33.
16. Tritton DJ (1988) *Physical Fluid Dynamics* (Oxford Science Publications, Oxford), pp 188–196.
17. Sano M, Wu XZ, Libchaber A (1989) Turbulence in helium-gas free convection. *Phys Rev A* 40(11):6421–6430.
18. Ciliberto S, Cioni S, Laroche C (1996) Large-scale flow properties of turbulent thermal convection. *Phys Rev E Stat Phys Plasmas Fluids Relat Interdiscip Topics* 54(6): R5901–R5904.
19. Sreenivasan KR, Bershadskii A, Niemela JJ (2002) Mean wind and its reversal in thermal convection. *Phys Rev E Stat Nonlin Soft Matter Phys* 65(5 Pt 2):056306.
20. Fischer PF (1997) An overlapping Schwarz method for Spectral Element Solution of the incompressible Navier-Stokes equations. *J Comput Phys* 133(1):84–101.
21. Scheel JD, Emran MS, Schumacher J (2013) Resolving the fine-scale structure in turbulent Rayleigh-Bénard convection. *New J Phys* 15:113063.
22. Yakhot V (2001) Mean-field approximation and a small parameter in turbulence theory. *Phys Rev E Stat Nonlin Soft Matter Phys* 63(2 Pt 2):026307.
23. Doering CR, Foias C (2002) Energy dissipation in body-forced turbulence. *J Fluid Mech* 467:289–306.
24. Doering CR (2009) The 3D Navier-Stokes problem. *Annu Rev Fluid Mech* 41:109–128.
25. Paladin G, Vulpiani A (1987) Degrees of freedom of turbulence. *Phys Rev A* 35(4): 1971–1973.
26. Sreenivasan KR, Meneveau C (1988) Singularities of the equations of fluid motion. *Phys Rev A* 38(12):6287–6295.
27. Polyakov AM (1995) Turbulence without pressure. *Phys Rev E Stat Phys Plasmas Fluids Relat Interdiscip Topics* 52(6):6183–6188.
28. Yakhot V, Sreenivasan KR (2005) Anomalous scaling of structure functions and dynamic constraints on turbulence simulations. *J Stat Phys* 121:823–884.
29. Kolmogorov AN (1962) A refinement of previous hypotheses concerning the local structure of turbulence in a viscous incompressible fluid at high Reynolds number. *J Fluid Mech* 13:82–85.
30. Stolovitzky G, Sreenivasan KR (1994) Kolmogorov's refined similarity hypothesis and general stochastic processes. *Rev Mod Phys* 66:229–240.
31. Wallace JM, Vukoslavcević PV (2010) Measurement of the velocity gradient tensor in turbulent flows. *Annu Rev Fluid Mech* 42:157–181.
32. Vincent A, Meneguzzi M (1991) The spatial structure and statistical properties of homogeneous turbulence. *J Fluid Mech* 225:1–20.
33. Kim J, Moin P, Moser RJ (1987) Turbulence statistics in fully developed channel flow at low Reynolds number. *J Fluid Mech* 177:133–166.
34. Flores O, Jimenez J, del Alamo JC (2007) Vorticity organization in the outer layer of turbulent channels with disturbed walls. *J Fluid Mech* 591:145–154.

PHYSICS